Proc. XIVth Int. Congr. on Rheology August 22-27, 2004
Edited by: Seoul, Korea

Numerical simulations of steady viscoelastic flow in a 4:1 square/square contraction

Manuel A. Alves[a], Fernando T. Pinho[b], and Paulo J. Oliveira[c]

[a]Departamento de Engenharia Química, Centro de Estudos de Fenómenos de Transporte, Faculdade de Engenharia da Universidade do Porto, 4200-465 Porto, Portugal
[b]Centro de Estudos de Fenómenos de Transporte, Departamento de Engenharia Mecânica, Universidade do Minho, 4800-058 Guimarães, Portugal
[c]Departamento de Engenharia Electromecânica, Unidade de Materiais Têxteis e Papeleiros, Universidade da Beira Interior, 6201-001 Covilhã, Portugal

ABSTRACT

Numerical simulations of the 3D steady flow in a 4:1 square/square sudden contraction were carried out for a Newtonian and a 4 mode PTT model representing a viscoelastic fluid. The simulations, all for conditions of negligible inertia, compared well with the experimental visualizations for both fluids. For the viscoelastic fluid an intense vortex enhancement was observed, and an elastic reversal of flow pattern within the recirculations relative to that for Newtonian fluids was predicted in the numerical simulations, in agreement with the experimental visualizations.

INTRODUCTION

Sudden contraction flows are classical benchmark problems in computational rheology [1] and possess features found in many industrial flows. Consequently, a large number of experimental and numerical investigations have been carried out over the years for the planar and circular cases.
For 3D contractions much less has been done, and this works presents new results of numerical simulations that correspond to experimental results presented also at this conference [2].
As far as we are aware, the first work on square contractions was by Walters and Webster [3] who found similarities with the flow through a circular contraction and these were indirectly confirmed by Walters and Rawlinson [4]. In terms of numerical work, the literature is scarcer; the 3D flows investigated usually contract only in one direction [5-7], and the simulations can hardly be considered as representative of actual 3D flows.

GOVERNING EQUATIONS

The equations to be solved are the continuity (Eq. 1), momentum (Eq. 2), and a constitutive equation for the polymer stress τ_{ij}

$$\frac{\partial u_j}{\partial x_j} = 0 \tag{1}$$

$$\rho\frac{\partial u_i}{\partial t} + \rho\frac{\partial (u_j u_i)}{\partial x_j} = -\frac{\partial p}{\partial x_i} + \eta_s \frac{\partial^2 u_i}{\partial x_j^2} + \frac{\partial \tau_{ij}}{\partial x_j} \tag{2}$$

In these equations u_i represents the velocity components, p the pressure and ρ the density. The stress field is expressed as the sum of a Newtonian solvent contribution of viscosity η_s and a polymer contribution, τ_{ij}.

The polymer contribution τ_{ij} is expressed as a sum of N viscoelastic modes (here N=4):

$$\tau_{ij} = \sum_{m=1}^{N} \tau_{ij,m} \tag{3}$$

each of which obeys a PTT equation,

$$Y(\tau_{kk,m})\tau_{ij,m} + \lambda_m \left(\frac{\partial \tau_{ij,m}}{\partial t} + \frac{\partial (u_k \tau_{ij,m})}{\partial x_k} \right) =$$
$$\eta_m \left(\frac{\partial u_i}{\partial x_j} + \frac{\partial u_j}{\partial x_i} \right) + \lambda_m \left(\tau_{jk,m} \frac{\partial u_i}{\partial x_k} + \tau_{ik,m} \frac{\partial u_j}{\partial x_k} \right) - \tag{4}$$
$$\lambda_m \frac{\xi}{2} \left[\tau_{jk,m} \left(\frac{\partial u_i}{\partial x_k} + \frac{\partial u_k}{\partial x_i} \right) + \tau_{ik,m} \left(\frac{\partial u_j}{\partial x_k} + \frac{\partial u_k}{\partial x_j} \right) \right]$$

The linear stress coefficient was selected, thus

$$Y(\tau_{kk,m}) = 1 + \frac{\lambda_m \varepsilon}{\eta_m} \tau_{kk,m} \tag{5}$$

In the above equations λ_m stands for m-mode relaxation time and η_m for the polymer viscosity coefficient; in addition, ε and ξ are parameter coefficients of the PTT model that influence the extensional viscosity and the normal stress coefficients. In Eq. (4) the terms on the left-hand-side are treated implicitly in the numerical solution of the corresponding algebraic equations,

whereas those on the right-hand-side go to the source and are treated explicitly.

NUMERICAL METHOD

The sets of governing equations are solved with the finite volume method described in detail in Oliveira et al [8]. Basically, the solution domain is decomposed in a large number of adjacent control volumes over which those equations are integrated and transformed into algebraic form. These discretized matrix equations are then solved sequentially for each dependent variable (u, p, τ) with conjugate gradient solvers, and the inherent nonlinearities of the convective terms, and in the $Y(\tau)$ coefficient in the constitutive equation, are dealt with by iteration. The meshes are non-staggered, the full coupling between pressure, velocity and stress fields is ensured with a special interpolation method [9] and the SIMPLEC algorithm deals with pressure-velocity coupling.

For the multi-mode constitutive equation the changes in the algorithm are minor: instead of solving a single constitutive equation, the equations pertaining to the various modes are solved sequentially. Since it is the solution of the pressure correction equation that takes longer in the present numerical method, the increase in computational time associated with multimodes is marginal relative to the single mode case.

The discretization of the diffusive terms is done by central differences, a formally second order accurate scheme. For the convective terms, second or third order accuracy is achieved with the high-resolution scheme (CUBISTA) proposed by Alves et al [10].

FLUIDS SELECTED

The parameters of the models were selected so that they fit well the rheology of the fluids used by Alves [11]. The parameters are the following: for the Newtonian fluid $\eta_s = 0.43$ Pa.s at 18ºC, the temperature at which the visualizations took place. For the viscoelastic fluid a four mode PTT model was used, with the following parameters estimated from the rheological measurements in steady and oscillatory shear flow (15ºC): $\eta_s = 0.27$ Pa.s ; $\eta_1 = 2.5$ Pa.s ; $\eta_2 = 0.9$ Pa.s ; $\eta_3 = 0.3$ Pa.s ; $\eta_4 = 0.1$ Pa.s ; $\lambda_1 = 30$ s ; $\lambda_2 = 3$ s ; $\lambda_3 = 0.3$ s ; $\lambda_4 = 0.03$ s ; $\varepsilon = 0.02$; $\xi = 0.04$.

With these parameters the constitutive equation represents well the linear viscoelastic spectrum and the steady shear behavior assessed in terms of shear viscosity and first normal stress difference coefficient. For other temperatures the time-temperature superposition principle can be used, with the shifting factor defined in terms of an Arrhenius equation,

$$\ln(a_T) = \ln\left[\eta_0(T)/\eta_0(T_0)\right] = 5900\left(1/T - 1/T_0\right) \quad (6)$$

valid for the absolute temperature range between 283.15 K and 303.15 K. The reference temperature in Eq. (6) is $T_0 = 288.15$ K .

RESULTS

All simulations were carried out at very low Reynolds numbers (in agreement with the experiments), here defined in terms of upstream quantities, $Re = \rho U_1 H_1 / \eta$. The flow elasticity is quantified with the Deborah number, here defined as $De = \lambda_p U_1 / H_1$, where λ_p represents the relaxation time, calculated from the linear viscoelastic spectrum via

$$\lambda_p = \sum_{m \neq \text{solvent}} \eta_m \lambda_m / \eta_p \ ; \ \eta_p = \sum_{m \neq \text{solvent}} \eta_m \qquad (7)$$

Figure 1 shows the excellent agreement between the measured and calculated streaklines for the Newtonian fluid at creeping flow conditions (Re=0.0085). It is necessary to increase the Reynolds number to 0.1 in order to observe a reduction in recirculation length of about 8%.

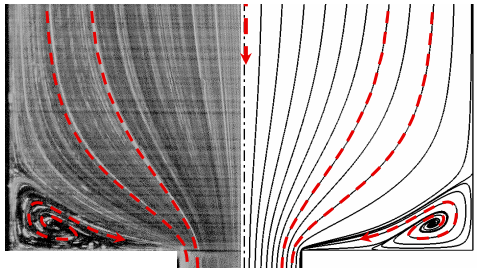

Figure 1. Comparison between experimental and predicted streamlines in the middle plane (Re=0.0085).

An interesting feature seen in Figure 1 is that the vortices are not closed. In fact there is an intricate interaction between the flows in the middle and diagonal planes, as illustrated in Figure 2.

For the viscoelastic fluid we were able to predict the flow patterns up to $De \approx 1$, with good quantitative agreement, in terms of vortex length, up to De=0.7. This is clearly seen in Figure 3, representing the variation with the Deborah number of the middle plane vortex length, x_R / H_1, and in the streamline comparison presented in Figure 4. Further comparisons can be found in [11].

The first and expected effect brought about by elasticity is that of enhancing the size of the vortex, but a second unexpected change can be

seen in Figure 5: the complete reversal of the fluid particle trajectories due to the interaction between the middle-plane and corner-plane vortices, relative to what was illustrated in Figure 2 for Newtonian fluids (also compare Figures 1 and 4). More details can be found in [11].

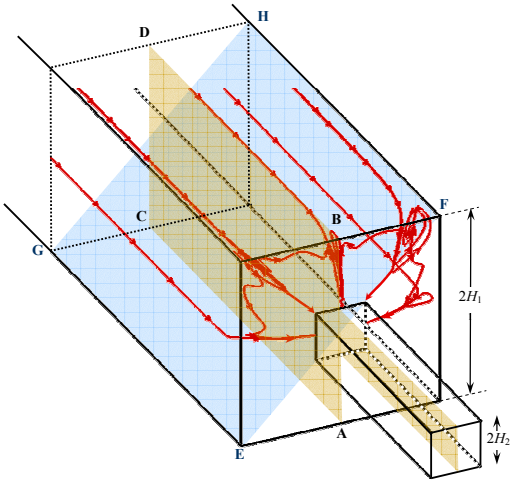

Figure 2. Predicted 3D pathlines for the Newtonian fluid under creeping flow conditions.

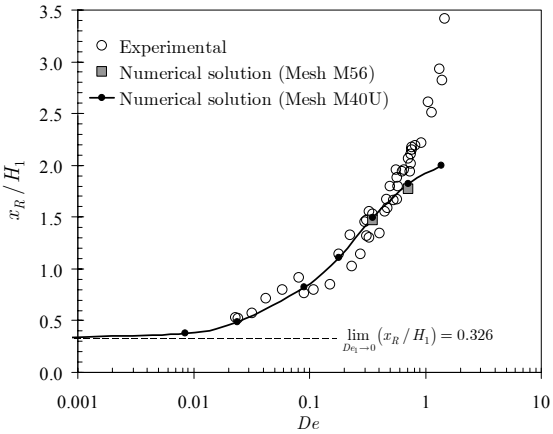

Figure 3. Comparison between the experimental and numerical results of the vortex length, x_R/H_1, for the viscoelastic fluid.

REFERENCES

1. Hassager O, J. Non-Newt. Fluid Mech., **29**, 2 (1988).
2. Alves MA, Pinho FT and Oliveira PJ, Proc. XIVth Int. Congr. on Rheology, Korea (2004).
3. Walters K and Webster MF, Phil. Trans. R. Soc. London A, **308**, 199 (1982).
4. Walters K and Rawlinson DM, Rheol. Acta, **21**, 547 (1982).
5. Mompean G and Deville M, J. Non-Newt. Fluid Mech., **72**, 253 (1997).
6. Xue SC, Phan-Thien N and Tanner RI, J. Non-Newt. Fluid Mech., **74**, 195 (1998).
7. Xue SC, Phan-Thien N and Tanner RI, Rheol. Acta, **37**, 158 (1998).
8. Oliveira PJ, Pinho FT and Pinto GA, J. Non-Newt. Fluid Mech., **79**, 1 (1998).
9. Oliveira PJ e Pinho FT, Num. Heat Transfer B, **35**, 295 (1999).
10. Alves MA, Oliveira PJ and Pinho FT, Int. J. Num. Methods in Fluids, **41**, 47 (2003).
11. Alves MA, Laminar flows of viscoelastic fluids: numerical, theoretical and experimental analysis (in Portuguese). PhD Thesis, Universidade do Porto, Portugal (2004).

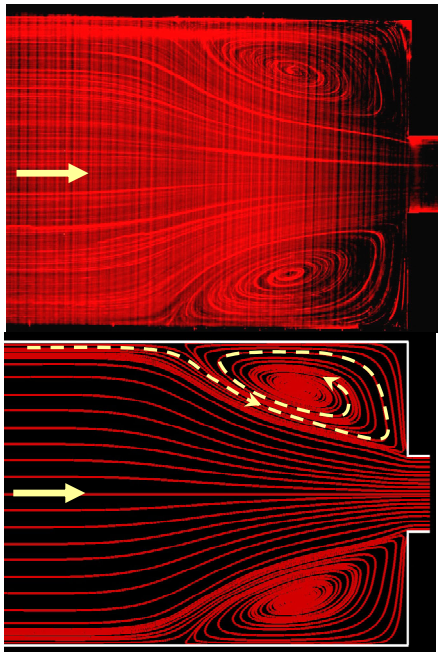

Figure 4. Comparison between the experimental streamlines (top) in the middle plane and the numerical predictions (bottom) for the viscoelastic fluid at De_1=0.355.

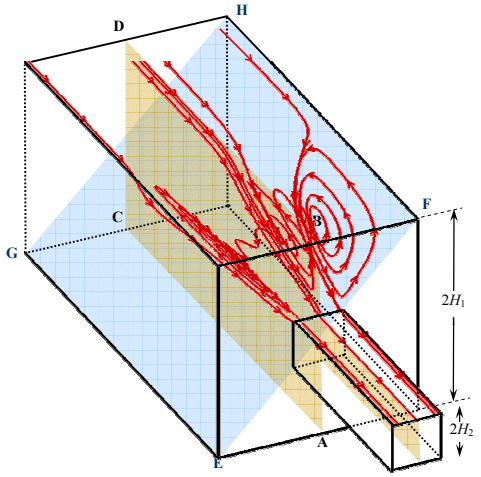

Figure 5. Predicted 3D pathlines for the viscoelastic fluid under creeping flow conditions.